J Mater Sci (2007) 42:5431–5436
DOI 10.1007/s10853-006-0826-9

Effect of grain width and aspect ratio on mechanical properties of Si_3N_4 ceramics

Zoran Krstic · Zhengbo Yu · Vladimir D. Krstic

Received: 23 October 2005 / Accepted: 21 August 2006 / Published online: 29 March 2007

Abstract Sintering additives Y_2O_3 and Al_2O_3 with different ratios ((Y_2O_3/Al_2O_3) from 1 to 4) were used to sinter Si_3N_4 to high density and to induce microstructural changes suitable for raising mechanical properties of the resultant ceramics. The sintered Si_3N_4 ceramics have bimodal microstructures with elongated β-Si_3N_4 grains uniformly distributed in a matrix of equiaxed or slightly elongated grains. Pores were found within the grain boundary phase at the junction regions of Si_3N_4 grains. The highest average aspect ratio (length/width of the grains) of ~4.92 was found for Y_2O_3/Al_2O_3 ratio of 2.33 with fracture toughness and strength values of ~7 MPam$^{1/2}$ and 800 MPa, respectively. The effect of microstructure, specifically grain morphology, on mechanical properties of sintered Si_3N_4 were investigated and found that the aspect ratio of the elongated grains is the most important microstructural feature which controls mechanical properties of these ceramics.

Introduction

Evolution of microstructure during sintering of Si_3N_4 and its effect on mechanical properties has been one of the main topics of numerous studies over the last number of years [1–8]. The properties of Si_3N_4 ceramics strongly depend on the microstructure developed during different sintering conditions, therefore microstructural design is a key factor in optimization of processing parameters and mechanical properties of Si_3N_4 ceramics.

Z. Krstic (✉) · Z. Yu · V. D. Krstic
Mechanical and Materials, Queen's University, 60 Union st, Kingston, ON, Canada K7M 1B5
e-mail: krstic@me.queensu.ca

The amount of sintering aids used affects the density of the ceramics [9] and the chemical composition of the grain boundary phase. The chemistry of the liquid phase, formed between sintering aids and oxide layer (SiO_2) on the surface of the Si_3N_4 particles, along with characteristics of the sintering powder and processing conditions, are the key factor in determining the microstructure and mechanical properties of Si_3N_4 ceramics [9].

Woetting and Ziegler [10] in 1984 showed that the presence of Al_2O_3 and Y_2O_3 has a strong effect on density and grain shape and any increase of Y_2O_3 concentration leads to an increase in liquidus temperatures and thus to viscosities at the sintering temperature. The development of elongated β-Si_3N_4 depends mainly on the diffusion rate during α to β phase transformation, and on the viscosity of the liquid at the sintering temperature. The higher the viscosity the lower the diffusion rates and thus the higher the aspect ratio of β-Si_3N_4 elongated grains will be. The aspect ratio is defined as [11]

$$\begin{aligned} \mathrm{AR} = \frac{L}{W} &= \left(\frac{K_L^{1/3}}{K_W^{1/5}}\right) \cdot t^{(1/3-1/5)} = \left(\frac{K_L^{1/3}}{K_W^{1/5}}\right) \cdot t^{(2/15)} \\ &= \left(\frac{K_{OL}^{1/3}}{K_{OW}^{2/15}}\right) \cdot t^{(2/15)} \exp\left[\frac{\left(\frac{Q_L}{3} - \frac{Q_W}{5}\right)}{RT}\right] \end{aligned} \quad (1)$$

where L is the average length of the β-Si_3N_4 grains, W is the average width of the β-Si_3N_4 grains, K_L and K_W are the rate constants in the length and width direction of the β-Si_3N_4 grains, Q_L and Q_W are the activation energies for length and width respectively, R is the gas constant, t is the time and T is the absolute temperature. Due to prismatic configuration of β-Si_3N_4 grains, the growth of length in the c direction [0001] is controlled mainly by the solute diffusion through multigrain junctions, while the growth of width in the [2100] direction is controlled by the diffusion along grain boundaries. According to this, the growth rate in the width direction is lower than the growth in the length direction resulting in the formation of elongated β-Si_3N_4 grains.

These elongated grains produced in the same matrix material have an important role in toughening of Si_3N_4 ceramics. The two most important mechanisms of toughening in this self-reinforced or in situ reinforced Si_3N_4 ceramics are crack bridging and crack deflection. In order for crack bridging to occur, the microstructure must consist of rod-like β-Si_3N_4 elongated grains uniformly distributed in a matrix of smaller either slightly elongated or equiexed grains. These two mechanisms contribute to enhanced energy dissipation upon crack propagation and hence can result in increase fracture toughness [12]. It should be noted that a weak interface between the elongated grains and surrounding intergranular phase are generally required for these two toughening mechanisms to operate. The resulting fracture toughness of monolithic Si_3N_4 ceramics is reported in the literature to be mainly governed by the morphology of the Si_3N_4 grains, i.e., the grain diameter and aspect ratio of the grains [12–14]. Faber and Evans [15] developed a model for toughening mechanism by crack deflection which relates fracture toughness and aspect ratio. In that model, any increase in aspect ratio of the rod shape reinforcing particles increases fracture toughness. Correlation between the square root of the average grain diameter and fracture toughness, and a linear relationship between aspect ratio of the elongated Si_3N_4 particles and fracture toughness was observed by Mitomo and Uenosono [16]. In their study no conclusion was drawn whether the aspect ratio or grain diameter is the dominant parameter in controlling fracture toughness.

Kawashima et al. [14] and Mitomo [17] showed that the fracture toughness of silicon nitride depends on the diameter of the larger elongated grains. Becher et al. [18] presented a model which relates the fracture toughness to the diameter of the bridging grains according to following equation:

$$K_{IC} = \left\{(\sigma_r)^2 d_W f \gamma_r E_c / 24 E_r \gamma_i\right\}^{1/2} \tag{2}$$

where σ_r is the tensile strength of the elongated grain, d_W is the diameter of the elongated grains, f is the volume fraction of the bridging grains, γ_r and γ_i are the fracture energy and interfacial debonding energy, respectively. E_r and E_c are the Young's moduli of the reinforcing phase and composite, respectively.

In the case of whiskers or elongated grains pullout the resultant toughening contribution is also expressed in terms of grain diameter using equation:

$$K_{IC} = \left\{(\sigma_r)^3 d_W f \gamma_r E_c / 12 E_r \tau_i\right\}^{1/2} \tag{3}$$

where σ_r, d_W, f, γ_r, E_r and E_c have the same meaning as in Eq. (2), and τ_ι is the shear resistance of the interface. In Eq. (3) the fracture toughness is predicted to increase with whiskers content and whiskers diameter. Kleebe et al. [12] reported a continuous increase of fracture toughness for Si_3N_4 with grain diameter. However, no relationship was developed which relates toughness to the aspect ratio. Recently, Krstic [7] has developed a model which relates fracture toughness to the aspect ratio of the elongated grains. In addition to aspect ratio, the volume fraction of elongated grains plays equally important role as expressed by the equation [7]:

$$K = K_m(1 - V) + \left\{4E\tau V u / \left(1 - v^2\right) K_m\right\} \cdot s \tag{4}$$

The model relates the fracture toughness to the pullout length u, the sliding friction stress τ, the grain aspect ratio s and the elongated grain volume friction V.

In Eq. (4) K is the stress intensity factor of the system, K_m is the critical stress intensity factor of the fine grain matrix, E is the Young's modulus and v is the Poison's ratio.

This paper presents a systematic study of the effect of elongated β-Si_3N_4 grain morphology on mechanical properties of silicon nitride ceramics especially fracture toughness and fracture strength. Another goal of the paper is to determine which microstructural feature is the dominant factor which controls toughening mechanisms in Si_3N_4 ceramics.

Experimental procedure

High purity, fine α-Si_3N_4 powder (Ube Industries E-10) was used as a raw material. Alumina (Alcoa A16-SG) and submicron size Y_2O_3 (Alpha Aesar) powders were used as sintering aids. Five different compositions have been prepared with different Y_2O_3/Al_2O_3 ratio (1, 1.5, 2.33, 3, and 4) but keeping constant amount of oxides (Y_2O_3 + Al_2O_3). Compositions were mixed for 12 h by ball-milling with alumina balls. This intensive milling procedure added 0.4 wt.% Al_2O_3 through the wear of the balls. Polyethylene glycol (PEG) was used as a binder, and after mechanical and isostatic pressing pressureless sintering was carried out in a graphite resistance furnace at temperatures ranging from 1,700 to 1,820°C for 1 h. The atmosphere in the furnace was the flowing N_2 gas. Four point-flexural strength testing was carried out on a jig with an inner and outer span of 20.00 and 40.00 mm, respectively. The cross-head speed was 0.003 mm/min. Ten samples were tested for each composition. Fracture toughness measurements were carried out using Vickers's indentation method at loads varying from 20 to 30 kg. The fracture toughness values were calculated using the following equation [19]

$$K_{IC} = 0.016 \cdot \left(\frac{E}{H}\right)^{0.5} \cdot \frac{P}{c^{1.5}} \tag{5}$$

where H is the hardness, E is the Young's modulus, P is the load and c is the crack length.

The Young's moduli of the samples were measured using an impulse-excitation of vibration technique (Grando-Sonic MK5, J.W Lemmens, INC. St. Louis MO USA) according to ASTM standards C 1259–94.

For microstructural analysis, the samples were first polished and then chemically etched with NaOH at 350°C for 130 s. Optical microscopy was used to examine polished and chemically etched surfaces. Scanning Electron Microscope (SEM) (Model JSM 840, Jeol Ltd., Tokyo, Japan) was employed to study the microstructure with an acceleration voltage of 20 KV. UTHSCSA 3.00 *Image Tool* was used as a software for microstructural analysis. It is based on ''Area analysis'' in which the volume fraction occupied by a certain phase is approximately equal to the portion of the surface occupied by the same phase in a section surface, provided that the particles are randomly distributed. For each composition section surface has taken from three different directions.

Results and discussion

The microstructure of sintered Si_3N_4 consists of bi-modal grains separated by glassy grain boundary phase. Figures 1, 2 and 3 show the effect of Y/A (Y_2O_3/Al_2O_3) ratio on grain morphology and grain size. For example, elongated grains in the composition Y/A ratio of 2.33 (Fig. 2) have the highest aspect ratio of ~4.92, while composition with Y/A ratio of 4 gave the highest width of the grains ~0.8 μm (Fig. 3). The highest density but lowest aspect ratio and width of the grains was observed for composition with Y/A ratio of 1 (Fig. 1). Figures 4 and 5 show the fracture surface of samples with Y/A ratios of 1 and 2.33, respectively. The samples exhibit mostly intergranular fracture with some indication for elongated grain pull-out (see arrows in Figs. 4 and 5).

The effect of average aspect ratio on fracture strength for different Y/A ratios is shown in Fig. 6. Clearly, the addition of Y_2O_3 increases the aspect ratio of the Si_3N_4 grains reaching the highest value of ~4.92 at Y/A ratio of 2.33. Also, according to Fig. 6 any increase in average aspect ratio leads to an increase in strength of Si_3N_4.

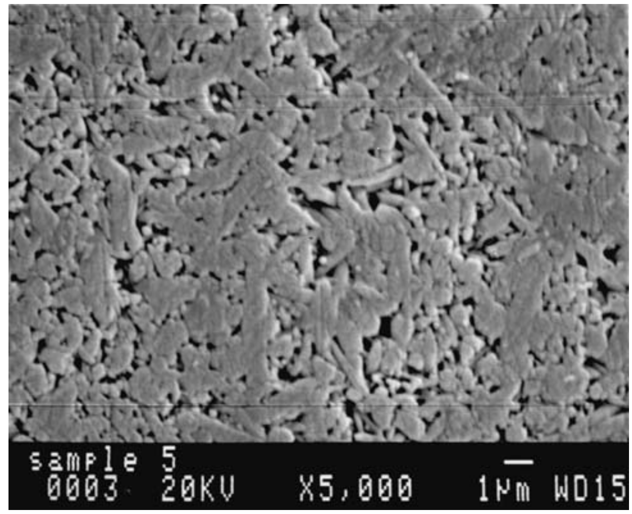

Fig. 1 Microstructure of sample with Y/A ratio of 1

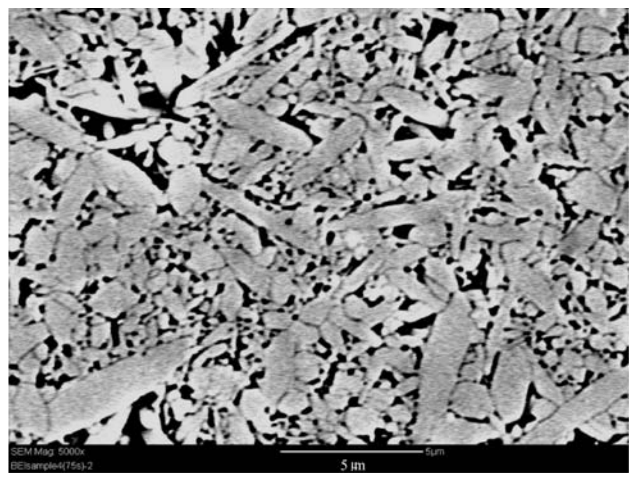

Fig. 2 Microstructure of sample with Y/A ratio of 2.33 (BSE mode)

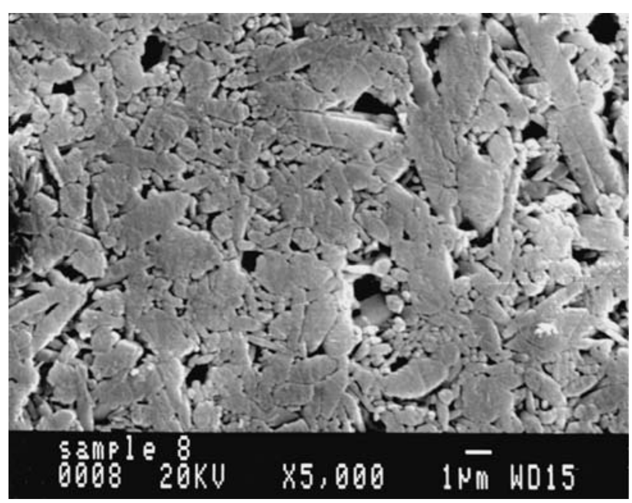

Fig. 3 Microstructure of sample with Y/A ratio of 4

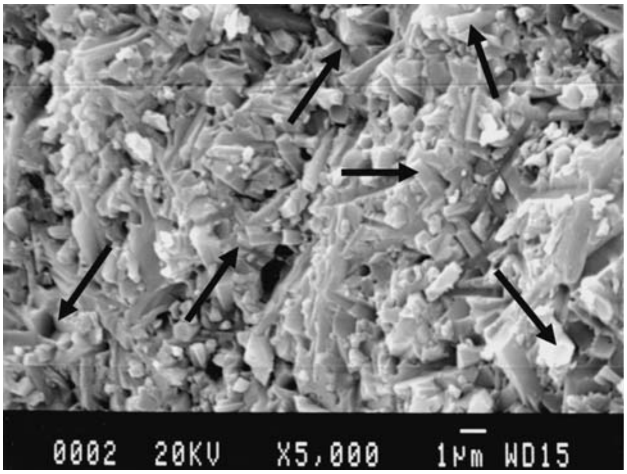

Fig. 4 Fracture surface of sample with Y/A ratio of 1

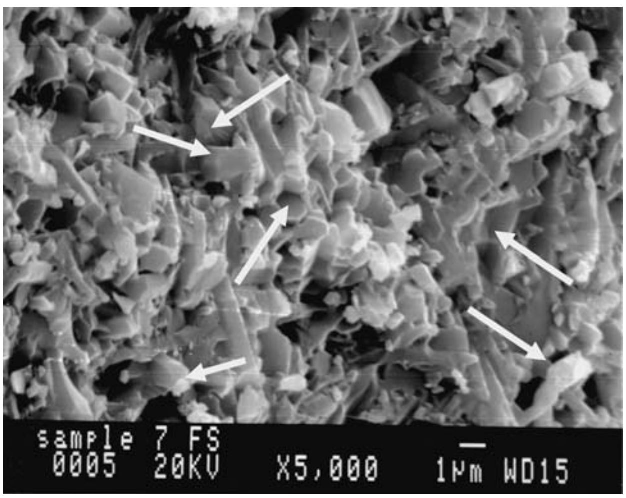

Fig. 5 Fracture surface of sample with Y/A ratio of 2.33

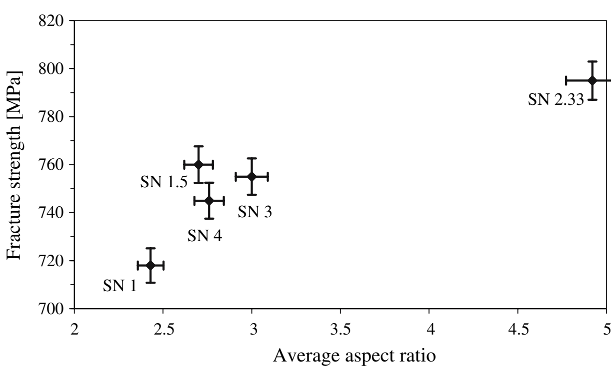

Fig. 6 Effect of average aspect ratio on strength for Y/A ratios

However, as the aspect ratio is increased there is an increase in the level of porosity (Ins. of Figs. 1–3), which in turn leads to a decrease in strength as shown in Fig. 6. Based on Figs. 1–3 and 6 the dominant mechanism of strengthening for samples with Y/A ratio of ≤2.33 is crack bridging by the elongated β-Si_3N_4 grains and associated crack deflection. However, for Y/A ratios >2.33 the dominant factor controlling the strength is porosity.

For fracture toughness determination, both the grain width and grain length were measured. Figures 7 and 8 show the change of fracture toughness with length and width of the grains, respectively. A continuous increase in fracture toughness with length of the grain is observed for all Y/A ratios. According to the Fig. 7 the highest fracture toughness was observed in samples with highest grain length. However, different relationship was found for the effect of grain width on the fracture toughness as shown in Fig. 8.

Figure 8 shows that the largest width of the grain does not coincide with the highest fracture toughness suggesting that the grain width alone does not control the fracture toughness. The highest width of the grains (i.e. 0.8 μm), is found for Y/A ratio of 4, which is not the composition with the highest fracture toughness. The lowest width of the grains of 0.6 μm was found in samples with Y/A ratio of 1 and this sample exhibits the lowest fracture toughness. This behavior is in agreement with Eq. (4) which predicts that the grain aspect ratio is the key factor which controls the toughening and not the grain width alone. In order to test

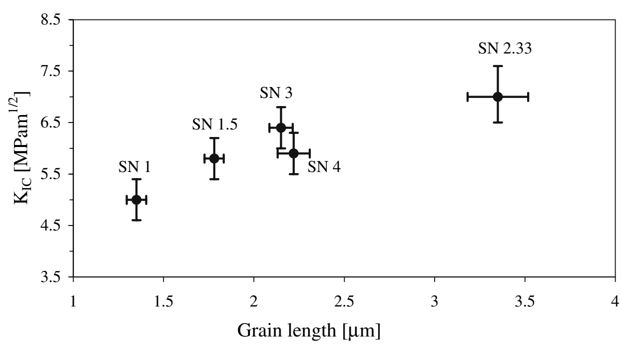

Fig. 7 Effect of average grain length on the fracture toughness for different Y/A ratios

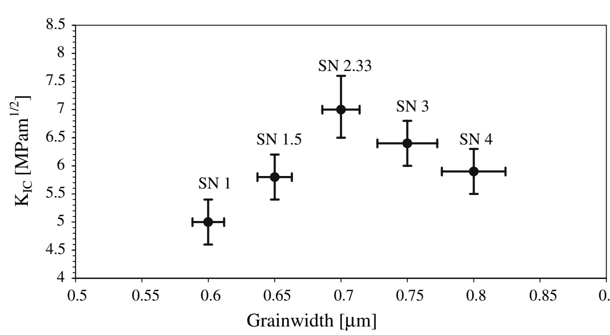

Fig. 8 Effect of average grain width on the fracture toughness for different Y/A ratios

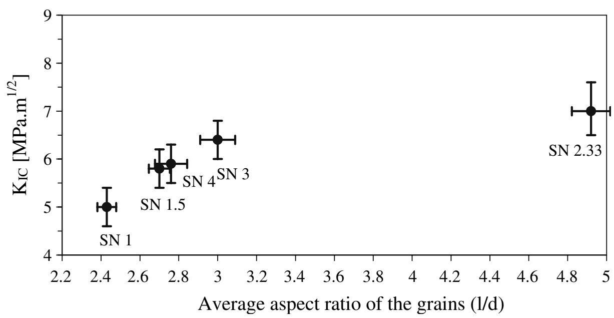

Fig. 9 Effect of average aspect ratio on the fracture toughness for different Y/A ratios

this prediction, a graph showing the change of K_{IC} as a function of aspect ratio was produced and presented in Fig. 9.

Although the relationship between fracture toughness and grain aspect ratio is not linear as predicted in Eq. (4), it does show that the aspect ratio controls the fracture toughness.

In developing the relationship between fracture toughness and grain aspect ratio in Fig. 9, the measurements were done only on grains with aspect ratios above ~1, without regard for the number or volume fraction of such grains. In order to determine the exact role of elongated grain volume fraction in toughening, the experimental measurements were done on samples with various Y/A ratios and the volume fraction was determined for grains with aspect ratio of over 5. This is an average aspect ratio between the smallest (~1) and largest (~11) elongated grain aspect ratios found in all samples. The results are presented in Fig. 10.

Figure 10 shows that the fracture toughness increases continuously with increasing of volume fraction of elongated grains. The highest value for toughness is found for volume fraction of elongated grains of ~22%, which is approximately one-third of the total elongated grains in the microstructure (all grains with aspect ratio of >1). This high volume fraction of grains with aspect ratio of >5 is found in samples containing higher amount of Y_2O_3 which confirms once again that yttria plays a critical role in enhancing the growth of elongated β-Si_3N_4 grains and thus in toughening.

The two strengthening and toughening mechanisms that operate most effectively in this system with elongated grains of high aspect ratio are crack deflection shown in Fig. 11 and crack bridging and pull-out shown in Fig. 12. One important conclusion that can be inferred from Figs. 6 and 9 is that both strength and toughness exhibit identical dependence on aspect ratio which indicates that the same mechanisms (Figs. 11 and 12) are responsible for both strengthening and toughening.

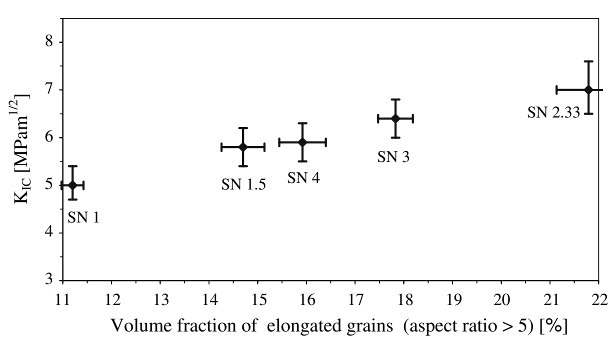

Fig. 10 Effect of the volume fraction of the elongated grains on the fracture toughness

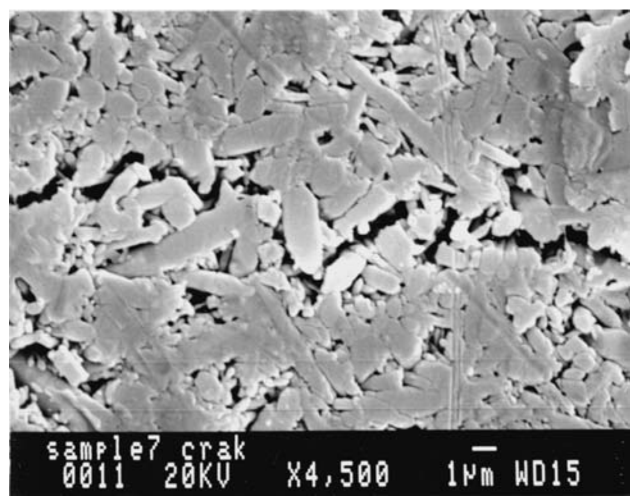

Fig. 11 Crack deflection in sample with Y/A ratio of 2.33

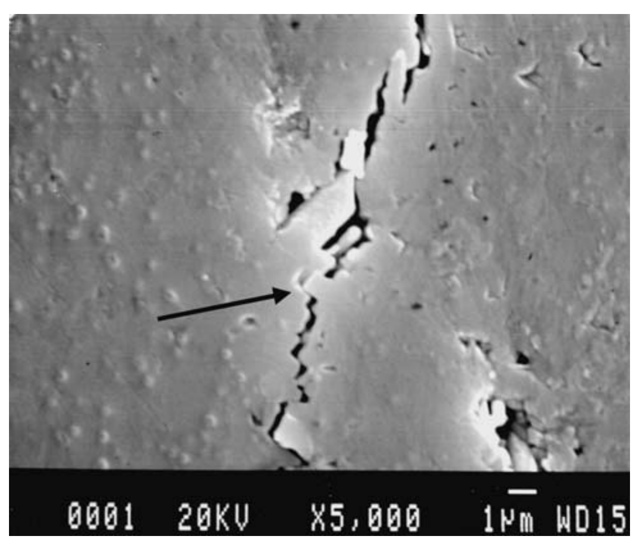

Fig. 12 Crack bridging and pull-out

Conclusion

It has been shown that the aspect ratio of the elongated grains plays the most important role in strengthening and toughening of Si_3N_4 ceramics. The maximum values for fracture toughness of 7 $MPam^{1/2}$ and strength 800 MPa, were obtained at the same Y/A ratio (2.33) suggesting that the same toughening mechanism(s) controls both the toughness and strength.

The microstructure of the sintered compacts consists mostly of β-Si_3N_4 elongated grains, with average aspect ratios between 2.35 and 4.92 uniformly distributed in the matrix of equiaxed or slightly elongated grains, separated by continuous oxide phases at the grain boundaries. Pores are located mainly within the oxide phase at the junction regions of the Si_3N_4 grains. Control of microstructure in Si_3N_4 is found to be a powerful method of imparting high fracture toughness and strength. The desirable microstructure that can offer high resistance to crack propagation is the one consisting of elongated grains in a matrix of equiaxed grains. The fracture toughness and strength of Si_3N_4 ceramics are controlled by the β-Si_3N_4 grain morphology and aspect ratio.

References

1. Trace RW, Halloran JW (1999) J Am Ceram Soc 82(10):2633
2. Li CW, Lee DJ, Lui SC (1992) J Am Ceram Soc 75(7):1777
3. Evans AG (1990) J Am Ceram Soc 73(2):187
4. Lange FF (1979) J Am Ceram Soc 62(7–8):428
5. Sajgalik P, Dusza J, Hoffman MJ (1995) J Am Ceram Soc 78(10):2619
6. Li C-W, Lui S-C, Goldacker J (1995) J Am Ceram Soc 78(2):449
7. Krstic VD (2000) In: Song J, Yin R (eds) Proceedings of international conference on engineering and technological science, vol 1. Chinese Academy of Engineering, Beijing, China, p 3
8. Liu X-J, Huang Z-Y, Pu X-P, Sun X–W, Huang L-P (2005) J Am Ceram Soc 88(5):1323
9. Krstic Z., Krstic VD (2003) Mater Sci Forum 413:129
10. Woetting G, Ziegler G (1984) Ceram Int 10(1):18
11. Tien TY (1995) In: Alper AM (ed) Study of silicon nitride ceramics, phase diagrams in advanced ceramics. Acadenic Press, San Diego, New York, Boston, USA, p 127
12. Kleebe H-J, Pezzotti G, Ziegler G (1999) J Am Ceram Soc 82(7):1857
13. Mitomo M, Uenosono S (1991) J Mater Sci 26:3940
14. Kawashima T, Okamoto H, Yamamoto H, Kitamura A (1991) J Ceram Soc Jpn 99(4):320
15. Faber KT, Evans AG (1983) Theory Acta Metall 31(4):565
16. Mitomo M, Uenosono S (1992) J Am Ceram Soc 75(1):103
17. Mitomo M (1991) In: Kimura S, Niihara K (eds) Proc. 1st Int. Symp. Sci. Eng. Ceram. Ceramic Society of Japan, Tokyo, p 101
18. Becher PF, Hwang S-L, Hsueh C-H (1995) MRS Bulletin/February, 23
19. Evans AG, Charles EA (1976) J\ Am Ceram Soc 59(7–8):371